CASCADE INJECTION PROCEDURE FOR BLADDER-ASSISTED RESIN TRANSFER MOLDING

C. Schillfahrt*, E. Fauster and R. Schledjewski

Processing of Composites Group, Department of Polymer Engineering and Science,
Montanuniversität Leoben, Otto-Glöckel Str. 2/III, 8700 Leoben, Austria
www.kunststofftechnik.at

*Corresponding author, e-mail: christian.schillfahrt@unileoben.ac.at

Keywords: Resin transfer molding, Bladder inflation molding, Cascade injection, Process analysis, Flow simulation

ABSTRACT

Hollow composite parts based on fiber reinforced plastics can be efficiently produced through bladder-assisted resin transfer molding (BARTM). The flow resistance of the textile reinforcements, however, limits the technical and economical manufacturability particularly for long composite structures, which is even more critical if fast curing or highly viscous resins are to be used. In order to overcome these process-inherent challenges, a cascade injection procedure for BARTM is investigated in this work. The basic idea of this approach is to considerably reduce flow lengths and thus total filling times. This is accomplished by a sequential filling of the part based on two or more injection points, which are located along the major axis of the part.

The following key issues are addressed in this paper, which are studied by means of flow simulations as well as saturation experiments on the basis of a specifically developed BARTM test rig. First, an optimal cascade injection scheme needs to be identified by evaluating filling times for different cascade injection scenarios. It is shown that shortest filling times can be achieved with a so-called cascaded central injection strategy. The next task implies an investigation of the system and process design of the injection setup, focusing on the configuration of injection gates, resin and venting lines and its effect on the filling behavior. In general, a ring gate has proved to be beneficial in contrast to a point gate, while the use of a venting line at the cascade injection point minimizes the risk of air entrapments in the laminate. The final objective comprises the realization of a fully automated cascade injection procedure. An efficient process control was implemented to enable an accurate switching of the individual injection cascades with respect to the changing filling state by using dedicated fluid detection sensors.

1 INTRODUCTION

Bladder-assisted resin transfer molding (BARTM) represents a suitable process technology for the production of longish and complex shaped hollow parts based on continuous fiber reinforced polymer composites [1]. Typical applications in automotive and aerospace industries are tube-like parts such as load-bearing frame structures or integral fluid piping elements (Figure 1). The basic process chain of the manufacturing process is depicted in Figure 2. Similar to any other liquid composite molding (LCM) process, it is based on the utilization of a dry textile preform. In case of BARTM, braided fiber reinforcements are typically used, which can directly be laid on an internal, inflatable mandrel by means of an over-braiding process [2,3]. Bladder and preform are then draped (if they don't have near-net-shape) and inserted into the cavity of a two-part mold. After closing the mold, the preform is compacted by applying a specific pressure to the inflatable bladder, which is followed by a pressure-controlled injection of the liquid matrix material. Lastly, the finished part is demolded as soon as the introduced resin is fully cured.

Figure 1: Complex shaped fluid piping elements for automotive application (Source: superTEX composites GmbH).

Resin injection is commonly conducted in the part's longitudinal direction, either from a central injection port or from end to end of the hollow part [3]. Due to the resistive nature of the textile reinforcements, a dominant portion of process cycle time is needed in the impregnation stage of the manufacturing process. This is particularly critical for long composite parts, as increasing flow lengths in pressure-controlled injections cause a disproportional growth of filling times. Hence, the use of fast curing or highly viscous resins can be significantly restricted, while the feasibility for series production of such components can be substantially limited. Furthermore, for parts exhibiting large flow lengths, the process-induced laminate thickness gradient at the end of the filling stage may not be sufficiently compensated anymore by subsequent consolidation or resin bleeding [2-5].

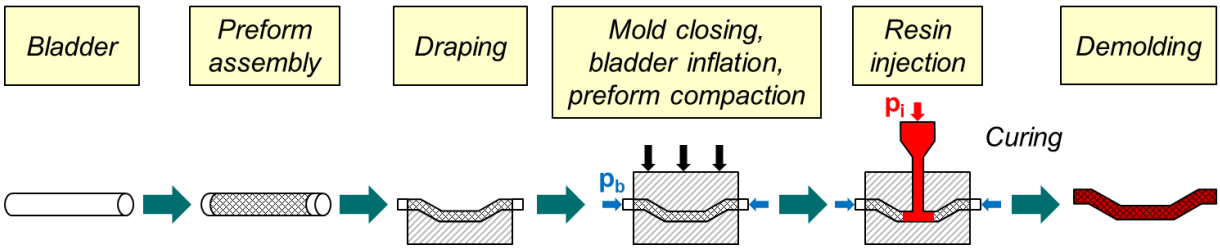

Figure 2: BARTM process chain.

In this work, a cascade injection concept for BARTM is studied to overcome the aforementioned difficulties associated with the manufacturing of long and hollow composite parts by reducing flow lengths and thus total filling times considerably. The basic principle of a cascaded injection process is to use two or more resin injection gates along the part's major axis in order to perform a sequential filling of the part sections [6-8]. However, the implementation of this injection strategy comes with various issues concerning the exact positioning of the injection points, the detection of the flow front and the subsequent switching of the resin gates. Thus, the following key tasks are investigated in this paper:

(1) Identification of an optimal cascade injection strategy by means of process analysis
(2) Investigation and evaluation of the process and system design of a cascaded BARTM concept
(3) Implementation of a fully automated cascade injection procedure at a BARTM test rig

2 PROCESS ANALYSIS

The first objective comprises the identification of an optimal cascade injection strategy, which is accomplished by comparing filling times from different injection scenarios based on an exemplary part geometry. By assuming a unidirectional fluid flow along the part's longitudinal axis, the impregnation process of a dry textile preform can be expressed with the one-dimensional form of Darcy's law [9]:

$$v_x = -\frac{k_{x,eff}}{\eta}\frac{dp}{dx}, \tag{1}$$

where v_x denotes the flow velocity of the impregnation liquid along the major axis of the part, which is dependent on the pressure gradient dp/dx at the flow front. The material parameters $k_{x,eff}$ and η correspond to the effective permeability of the preform and the dynamic viscosity of the resin, respectively. In BARTM processes, the permeability can be described by an apparent overall permeability $\tilde{k}_{x,eff}$ that is influenced by the non-linear preform compaction state during resin injection [4,10]. Filling times can be obtained by integrating Equation (1):

$$t_{f,i} = \frac{l_i^2\,\eta}{2\,\tilde{k}_{x,eff}\,\Delta p}, \tag{2}$$

where $t_{f,i}$ terms the filling time of part section i with length l_i and Δp is the constant pressure difference between the injection and outlet pressure. In order to obtain sequential filling of the part sections based on a cascaded injection scheme, individual resin gates are used that are positioned at the beginning of each section. Thus, the total part filling time t_f can be formulated as:

$$t_f = \sum_{i=1}^{n} t_{f,i}\,. \tag{3}$$

Filling time calculations were performed using a simple tubular part geometry with a diameter and length of 40 and 1000 mm, respectively (Figure 3). In order to investigate different cascade injection scenarios, the part was divided in up to four sections of equal length (strategies 1-4). These scenarios are compared to conventional injection procedures using only one resin gate at the part's end (state of the art 1) or center (state of the art 2). The used values for Δp, $\tilde{k}_{x,eff}$ and η were 1 bar, 1E-9 m² and 0.1 Pas. Besides analytical calculations, the flow simulation software PAM-RTM was used in conjunction with a tubular 2D surface mesh, comprising 2412 knots, 4800 elements and a segment length of 10 mm.

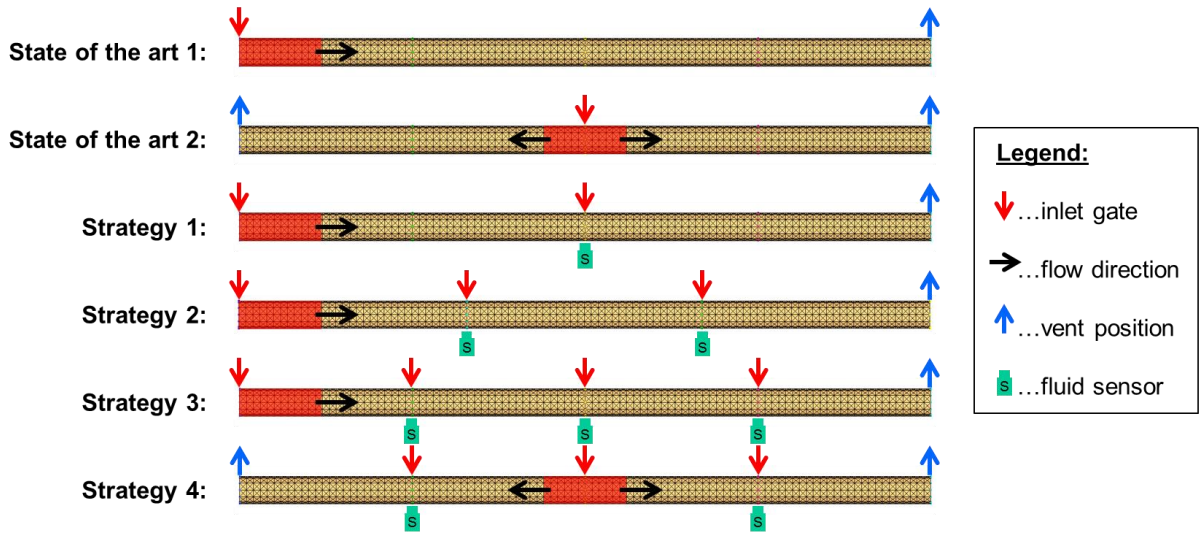

Figure 3: Identification of different injection strategies. Red and blue arrows depict inlet and vent positions, respectively, while S terms a fluid detection sensor required at each cascade injection gate.

The resulting filling times as well as the number of required flow front sensors are presented in Table 1. Although the absolute analytical and numerical results are slightly different, which was presumably caused by an influence of the used surface mesh, the outcome of the relative filling times with respect to the reference strategy is similar. It is clearly shown that the implementation of a central or cascaded injection procedure can lead to significantly reduced filling times. The lowest impregnation time was obtained by a so-called cascaded central injection (strategy 4). It can be seen as an optimal injection procedure for long composite parts and therefore is addressed in the following sections. Interestingly, in contrast to cascaded resin injections from the part's end, a conventional central injection is still beneficial as low filling times can be achieved with only one resin gate and without the use of any flow front sensors. However, in some cases the utilization of a cascaded injection offers advantages, e.g. if the resin gate cannot be positioned in the (possibly exposed) center of the part or if flow lengths have to be reduced to prevent segregation effects when using highly filled resin systems [11].

Injection strategy	# of fluid sensors	$t_{f,analytical}$ [s]	$t_{f,simulation}$ [s]	$t_{f,analytical}/t_{f,ref}$ [%]	$t_{f,simulation}/t_{f,ref}$ [%]
State of the art 1 (reference)	0	500	521	100	100
State of the art 2	0	125	129	25	25
Strategy 1	1	250	260	50	50
Strategy 2	2	167	173	33	33
Strategy 3	3	125	129	25	25
Strategy 4	2	63	64	13	12

Table 1: Resulting analytically and numerically calculated filling times and required number of fluid sensors for the identified injection strategies.

3 PROCESS AND SYSTEM DESIGN

In this section, the basic components of a cascaded central injection system and their influence on the flow behavior are investigated. This is achieved by numerical flow simulations and experimental investigations using a specifically developed saturation test rig for BARTM.

3.1 Test Rig

A saturation test rig for BARTM, which was developed in a previous study of the authors [10], was modified based on a symmetrical half-model of the cascaded central injection scheme presented in the last section (Figure 4). The setup comprises a transparent outer mold to allow for visual observation of the impregnation process, omitting the need for flow front sensors within experiments using manual process control. Different exchangeable injection gates can be applied at the cascade injection point in order to study their effect on the filling behavior. Colored corn oil is used as a substitutional impregnation liquid, which shows similar viscosity to common thermosetting injection resins. Process parameters such as injection and bladder pressure are centrally controlled by a specifically customized LabView application, while the saturation experiment can be recorded by an industrial camera system positioned above the assembly.

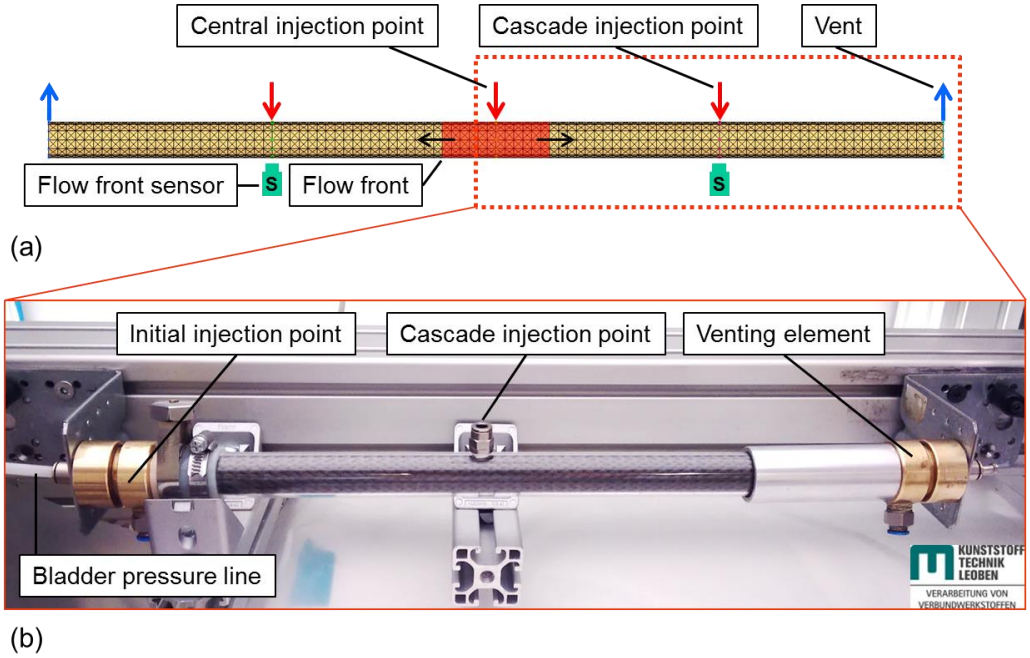

Figure 4: Designing a cascade injection setup for experimental investigations. (a) Flow simulation model of a cascaded central injection approach and (b) realized half-model implemented at a transparent BARTM test rig.

3.2 Central Injection Gate

The influence of the central injection port on the filling behavior is investigated by focusing on two different gate types: a ring gate and a point gate (Figure 5). While the former enables initial resin distribution around the part's circumference, which is then followed by a unidirectional fluid flow along the longitudinal axis of the part, the latter induces a two-dimensional resin flow in the preform that is dependent on its in-plane permeability characteristics. As this work focuses on symmetric biaxial braidings, it is assumed that the orientations of the principal permeabilities coincide with the preform's major axes (i.e. K1 in longitudinal and K2 in circumferential direction) [12]. Due to the complex fluid flow behavior when using point gates, filling calculations have to be performed using numerical flow simulations. On the other side, a point gate is beneficial in terms of tool complexity and reworking effort for removing the residual neat resin from the cured part surface.

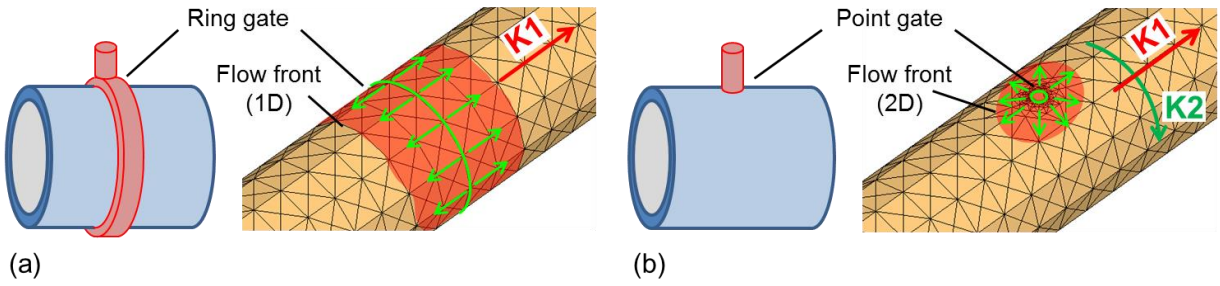

Figure 5: Identification of different resin gate designs and resulting flow front propagation during BARTM. (a) Ring gate and (b) point gate, which induce 1D and 2D resin flow, respectively.

Filling time calculations were conducted using PAM-RTM and the central injection model from the last section (state of the art 2). Besides the type of the ring gate, two further influencing factors were investigated: the preform permeability in circumferential direction for the cases K2=K1 (K2=1E-9 m²), K2>K1 (K2=1E-8 m²) and K2<K1 (K2=1E-10 m²) as well as the diameter of the point gate (4 and 8 mm). The obtained results are summarized in Table 2. As expected, the flow behavior using a ring

gate was independent of K2 due to the absence of any transversal fluid movement. In general, the utilization of a point gate led to a significant increase in filling times. Longer impregnation times were obtained for decreasing values for point gate diameter and permeability K2. Moreover, the influence of the point gate diameter was higher for smaller transversal permeability values.

Central injection gate	**K2=K1** $t_{f,simulation}$ [s]	**K2>K1** $t_{f,simulation}$ [s]	**K2<K1** $t_{f,simulation}$ [s]
Ring gate (reference)	129 (±0%)	129 (±0%)	129 (±0%)
Point gate (d=4mm)	178 (+38%)	142 (+10%)	309 (+140%)
Point gate (d=8mm)	162 (+26%)	136 (+5%)	254 (+97%)

Table 2: Resulting simulated filling times using different resin gates at the central injection port considering different preform permeabilities in circumferential direction.

Another aspect investigated for a central injection port equipped with a point gate is air entrapment. Figure 6 shows a qualitative comparison of flow simulation and saturation experiment for the critical case K2<K1. This constellation leads to long colliding flow fronts at the side opposite to the injection gate. Here, air in between the fluid fronts can easily be trapped and remain, which could be shown in the saturation experiments. Therefore it can be concluded that the utilization of a ring gate at the central injection port is highly beneficial for reducing filling times and part porosities.

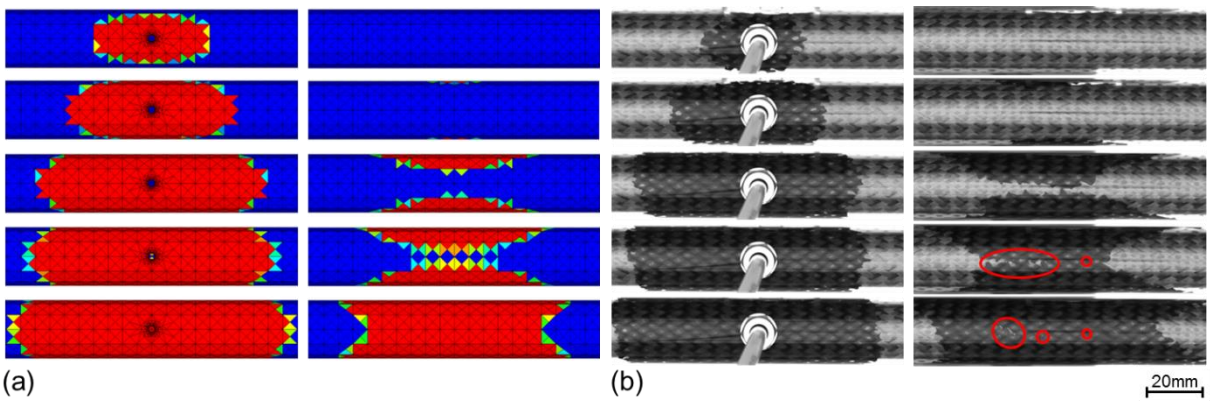

Figure 6: Qualitative comparison of the flow behavior in the vicinity of a central injection port based on a point gate, viewed from top (left) and from bottom (right). (a) Flow simulation and (b) saturation experiment (air entrapments are marked with red ellipses).

3.3 Cascade Injection Gate

Various influencing factors on the filling behavior can be identified regarding the cascade injection point and the switching of the resin ports. First, the utilization of a ring or point gate is possible here too. Furthermore, a venting system can be implemented at the cascade injection point for venting the injection line (Figure 7). This can avoid the introduction of air into the laminate when switching the resin gates. In this case, it is reasonable to position the flow front sensor behind the valve of the venting line instead of using an in-mold sensor. However, depending on the local flow resistances, it should be considered that the fluid could continue to flow in the next cascade during the filling of the venting system. A process-related influencing factor represents the switching procedure. While an opening of the cascade injection gate before the arrival of the flow front at this position can obviously lead to considerable air entrapment in the laminate and has therefore to be avoided by all means, a delayed switching results in decreased efficiency of the filling process. Another issue that needs to be investigated is the state of the initial injection gate during the filling of the second cascade.

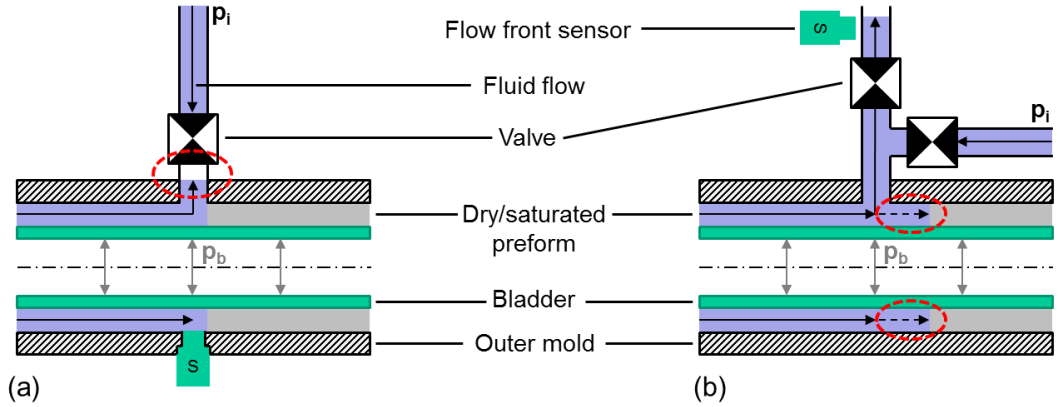

Figure 7: Different approaches for designing the cascade injection gate. (a) Injection gate without and (b) with venting line (potential problem zones are marked with red ellipses).

The aforementioned influencing factors were first examined by means of flow simulations using a simple cascade injection model from the first section (strategy 1) and neglecting the use of a venting system. Again, the effects of permeability in circumferential direction and point gate diameter were additionally considered. The resulting filling times shown in Table 3 are based on an accurate switching of the resin gates. The shortest impregnation times were obtained by the ring gate, which were invariant to the permeability K2 and to the state of the initial injection gate at the end of the part. In contrast, the use of a point gate still caused an increase in filling times, although this was less significant as it was for the central injection gate. Similar to the previous findings it could be shown that the case K2<K1 was the most critical and that an increasing point gate diameter led to a reduction in filling times. While here the state of the initial injection gate had negligible impact on the results for the cases K2=K1 and K2>K1, a little reduction in filling times was observed for the case K2<K1 when the initial gate was kept open.

Cascade injection gate	State of initial gate during filling of 2. cascade	**K2=K1** $t_{f,simulation}$ [s]	**K2>K1** $t_{f,simulation}$ [s]	**K2<K1** $t_{f,simulation}$ [s]
Ring gate (reference)	Closed or open	260 (±0%)	260 (±0%)	260 (±0%)
Point gate (d=4mm)	Closed	283 (+9%)	265 (+2%)	351 (+35%)
	Open	281 (+8%)	265 (+2%)	326 (+25%)
Point gate (d=8mm)	Closed	275 (+6%)	262 (+1%)	323 (+24%)
	Open	274 (+5%)	262 (+1%)	309 (+19%)

Table 3: Resulting computed filling times using different resin gates at the cascade injection point considering various preform permeabilities in circumferential direction as well as different states of the initial injection gate.

The next task was to verify the basic outcome of the flow simulations by means of saturation measurements using the adapted BARTM test rig (Figure 4). Moreover, the utilization of a venting system was considered. However, preliminary tests showed that when using a point gate, significant flow front advancement occurs during the filling of the venting system, while this wasn't observed for the ring gate, where the impregnation fluid solely entered the venting line (Figure 8). Thus, it was proposed to use a venting line only for a ring gate configuration in the following investigations. The saturation tests were conducted using a single layer of a biaxial braided sleeving based on 12K carbon fibers, a bladder pressure of 4 bar and an injection pressure of 1.5 bar. The resin gates were manually switched using ball valves at the injection and venting lines, while fluid arrival at the switching point was determined visually. In order to evaluate the potential for filling time reductions based on an application-oriented experiment, measurements were also performed using a conventional injection strategy (state of the art 1).

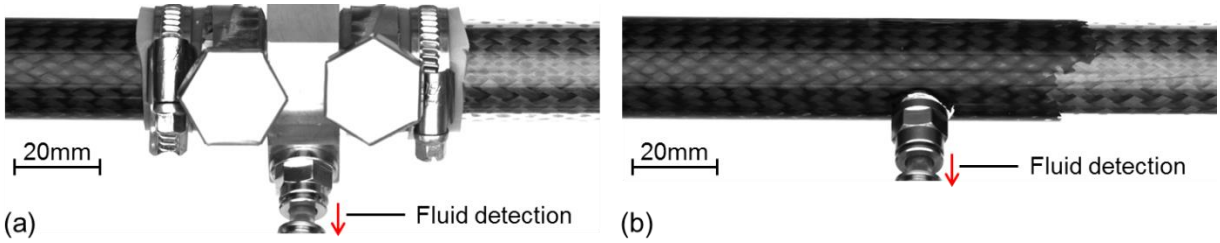

Figure 8: Preliminary saturation experiments using a venting line at the cascade injection point. (a) Ring gate: no fluid advancement in the second cascade (even long) after the filling of the venting line. (b) Point gate: continuing fluid flow in the preform.

The resulting filling times of the saturation experiments are summarized in Table 4. In case of the point gate setup, they reflect the basic outcome of the initial process analysis, as part filling times were significantly decreased using the selected cascade injection strategy. However, for the ring gate configuration, filling times were substantially higher, which was caused by the long filling time of the simple, but relatively oversized venting system prior to resin gate switching. Hence, the venting design needs to be optimized for future investigations, e.g. by reducing the filling volume of the venting system and by positioning the corresponding valve and fluid detection sensor as close as possible to the mold cavity. Interestingly, the filling times of the second cascade showed no significant influences from the resin gate type and from the initial injection gate state, considering the magnitude of typical process variabilities. Furthermore, a qualitative comparison between the filling simulations and the recorded flow front images showed good agreement, as exemplarily illustrated in Figure 9.

Cascade injection gate	State of initial gate during filling of 2. cascade	$t_{f,1.\&2.cascade}$ [s]	$t_{f,2.cascade}$ [s]
None (reference)	-	34,6	23,6
Ring gate with venting line	Closed	63,3 (+83%)	6,5 (-81%)
	Open	57,1 (+65%)	6,3 (-82%)
Point gate without venting line	Closed	17,2 (-50%)	7,0 (-80%)
	Open	16,8 (-51%)	6,8 (-80%)

Table 4: Measured filling times of conventional and cascaded BARTM saturation experiments using different resin gates and venting conditions at the cascade injection point as well as considering different states of the initial injection gate.

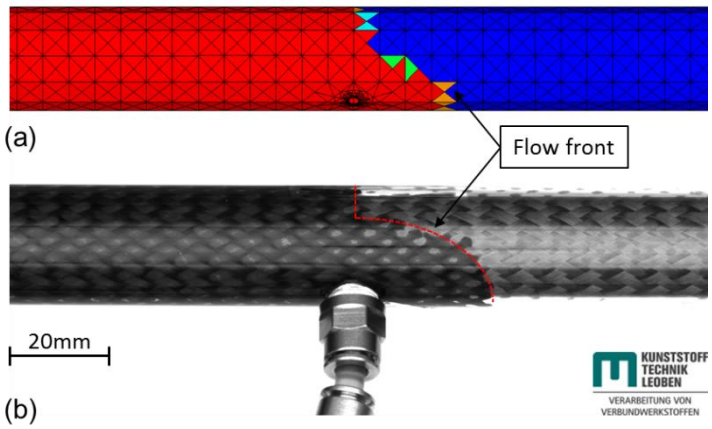

Figure 9: Filling behavior of a braided fabric after accurately switching the injection cascade and continuing the injection from a point gate onwards. Qualitative comparison of flow front images for (a) flow simulation and (b) saturation experiment.

Generally, good fabric saturation was obtained in the filling experiments by using the ring gate configuration and no air movement in the laminate was observed throughout the injection stage, which confirms the potential benefits of using a venting system. Moreover, the possibility of flushing the saturated cascade with fluid prior to resin gate switching could facilitate the removal of process-induced voids [13]. In contrast, the filling experiments using the point gate setup without venting line showed some air movement from the point gate in various directions after the switching, which could be attributed to the design of this configuration (Figure 7a). While some of these bubbles escaped at the fluid flow front in the second cascade, the rest of them were trapped in the initial part section and remained in the saturated laminate. This can be explained by a hypothetical pressure profile evolution at the cascade injection point, considering that air movement is driven by the locally acting pressure gradients (Figure 10).

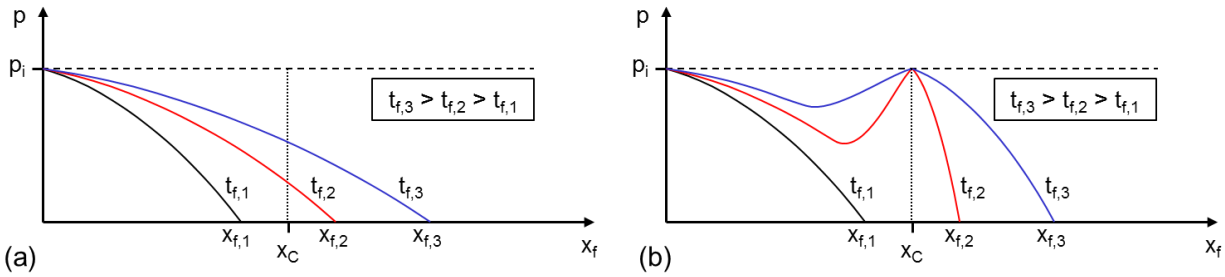

Figure 10: Schematic non-linear fluid pressure profiles in the vicinity of the cascade injection point x_C during BARTM with an applied injection pressure p_i. Comparison between (a) conventional and (b) cascaded injection process.

4 IMPELEMENTATION OF AN AUTOMATED CASCADE INJECTION SYSTEM

The final objective is the realization of a fully automated cascade injection procedure implemented at the BARTM test rig, which was specifically configured based on the previous findings (Figure 11). Although a simple cascade injection setup was chosen, it still represents a half-model of the optimal cascaded central injection strategy. The test rig was equipped with ring gates and a venting line at the cascade injection point. Solenoid valves were installed at each injection and venting line. While a pressure sensor was implemented near the initial injection port to monitor the fluid pressure, capacitive and photoelectric fluid detection sensors were used at the venting line in order to automatically trigger the switching of the resin gates. All peripheral equipment was connected to the LabView system, which was further modified to capture the timely advancing flow fronts in the corresponding cascades using digital image processing techniques.

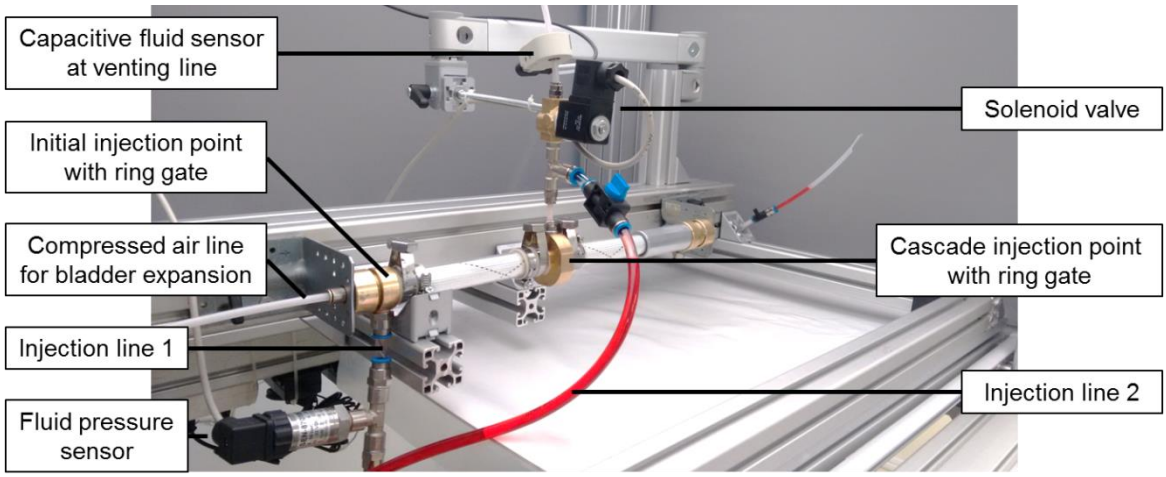

Figure 11: Modified test rig for investigating a fully automated, cascaded BARTM procedure.

Saturation experiments were conducted to investigate the repeatability of the automated injection procedure. Single layers of a braided sleeving comprising 300 tex glass fibers and a black tracer yarn for the detection of fabric distortions were used. The bladder pressure was 3.5 bar and the injection pressure was 2.0 and 2.5 bar, respectively. As there is still a considerable time for the filling of the venting system needed, the individual flow front profiles are evaluated with respect to the filling time after the opening of the corresponding injection gate (Figure 12). The repetitive measurements showed a fairly good agreement and gave distinctive flow front profiles for each injection pressure level. Considering the variability of the measurements, it can be concluded that it is highly beneficial to trigger the critical switching of the injection gates based on sensors signals instead of using a simple time control, which is the common practice in thermoplastic cascade injection molding processes [14].

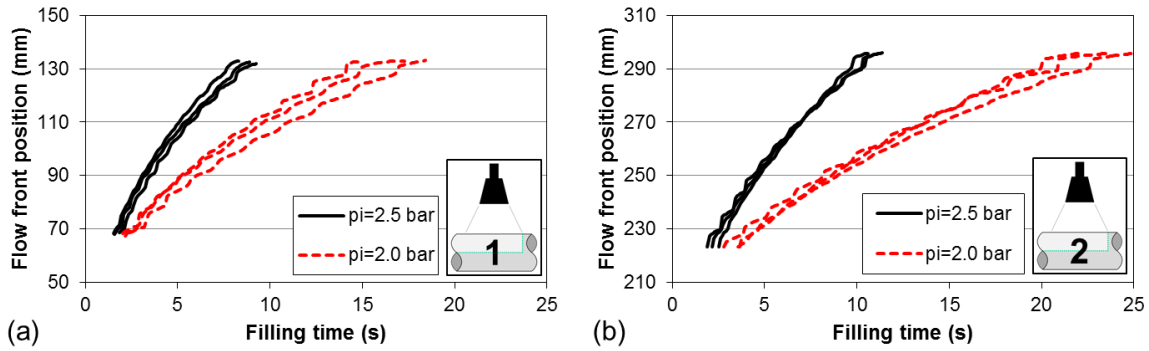

Figure 12: Obtained flow front positions over filling time. (a) Flow front profile in the first and (b) in the second cascade after opening the initial and central injection gate, respectively.

5 CONCLUSIONS

In this work, a cascade injection procedure for BARTM was investigated in order to overcome process-inherent limitations associated with the manufacturing of long and hollow composite parts. An initial process analysis showed that a considerable reduction of flow lengths and filling times can be achieved by application of a cascaded central injection scheme, meaning that the viscous matrix is introduced in the middle of the part with symmetrically positioned injection cascades on both sides. By using additional cascade injection points, part filling times can be flexibly adapted to technical or economical needs. However, a concurrent increase in system and process complexity should be considered too. An investigation of the process and system design showed that the utilization of a ring gate at the central injection port is highly beneficial as it enables shortest filling times in the first cascade and efficiently prevents the development of air entrapments. Furthermore, a ring gate induces linear flow fronts and the corresponding saturation behavior enables rather simple filling calculations, provided that the unidirectional, unsaturated apparent permeability of the preform is known. A major drawback is that due to the gate design a ring of neat resin will remain on the part surface being difficult to rework. Two different designs were proposed for the cascade injection points. The first one comprises the use of simple point gates without venting lines that are easy to integrate into the mold. Fluid detection is accomplished by means of in-mold flow front sensors. The second design involves the utilization of ring gates with venting lines in order to prevent any introduction of air into the cavity and to minimize the void content of the part. In this case, fluid detection sensors should be positioned at the venting lines. However, the efficiency of this concept is compromised due to the filling time of the venting system, which depends on its constructive design, and a possible flushing phase prior to the switching of the injection gates. Lastly, an exemplary approach for a fully automated cascade injection procedure using a modified BARTM test rig was presented. Accurate switching of the injection cascades was enabled through electronically controlled valves at the injection and venting lines, which were triggered by dedicated capacitive and photoelectric fluid detection sensors. Repetitive saturation experiments finally demonstrated the feasibility of the cascaded injection concept. Lastly it should be noted that when using thermosetting resins, curing of the matrix material in the injection and venting system must be avoided, which will be addressed in future investigations.

ACKNOWLEDGEMENTS

The authors kindly acknowledge the financial support received from the BMVIT and the Austrian Research Promotion Agency (FFG) in frame of the program "Production of the Future" within the research project "NovoTube" (contract no. 853453).

REFERENCES

[1] M. Neitzel, P. Mitschang and U. Breuer, *Handbuch Verbundwerkstoffe*, Hanser, München, 2014.

[2] U. Lehmann and W. Michaeli, Cores lead to an automated production of hollow composite parts in resin transfer moulding, *Composites Part A: Applied Science and Manufacturing*, **29**, 1998, pp. 803-810 (doi: 10.1016/S1359-835X(98)00007-4).

[3] U. Lehmann, *Herstellung von endlosfaserverstärkten, hohlen Formteilen mit innendruckbeaufschlagten Kernen im Harzinjektionsverfahren: Production of hollow composite parts with inflatable bladders in liquid composite moulding*, Verlag Mainz, Aachen, 1999.

[4] N.C. Correia, F. Robitaille, A.C. Long, C.D. Rudd, P. Šimáček and S.G. Advani, Use of Resin Transfer Molding Simulation to Predict Flow, Saturation, and Compaction in the VARTM Process, *Journal of Fluids Engineering*, **126**, 2004, pp. 210-215 (doi: 10.1115/1.1669032).

[5] P. Simacek, D. Heider, J.W. Gillespie and S. Advani, Post-filling flow in vacuum assisted resin transfer molding processes: Theoretical analysis, *Composites Part A: Applied Science and Manufacturing*, **40**, 2009, pp. 913-924 (doi: 10.1016/j.compositesa.2009.04.018).

[6] F. Flemming, G. Ziegmann and S. Roth, *Faserverbundbauweisen: Fertigungsverfahren mit duroplastischer Matrix*, Springer, Berlin, 1999.

[7] M. Henne and W. Buerzle, Maßnahmen zur Reduktion der Formfüllzeit - Teil 2, *Kunststoffe-Synthetics*, **53**, 2006, pp. 59-62.

[8] M. Hintermann, *Erforschung eines neuen Injektionsprozesses für offene und geschlossene Faserverbund-Strukturen*, PhD thesis, ETH Zürich, Zürich, 1998.

[9] H. Darcy, *Les Fontaines Publiques de la Ville de Dijon*, Victor Dalmont, Paris, 1856.

[10] C. Schillfahrt, E. Fauster and R. Schledjewski, Optical Permeability Measurement on Tubular Braided Reinforcing Textiles, *Proceedings of the 20th International Conference on Composite Materials ICCM20 (Eds. O.T. Thomsen, C. Berggreen, B.F. Sørensen), Copenhagen, Denmark, July 19-24, 2015*, Paper 3406-2, pp. 1-12.

[11] Y. Tang, L. Ye, D. Zhang and S. Deng, Characterization of transverse tensile, interlaminar shear and interlaminate fracture in CF/EP laminates with 10 wt% and 20 wt% silica nanoparticles in matrix resins, *Composites Part A: Applied Science and Manufacturing*, **42**, 2011, pp. 1943-1950 (doi: 10.1016/j.compositesa.2011.08.019).

[12] A. Endruweit and A.C. Long, A model for the in-plane permeability of triaxially braided reinforcements, *Composites Part A: Applied Science and Manufacturing*, **42**, 2011, pp. 165-172 (doi: 10.1016/j.compositesa.2010.11.003).

[13] S. Advani and E.M. Sozer, *Process Modeling in Composites Manufacturing*, CRC Press, Boca Raton, 2010.

[14] S. Berz, M. Carvani, Intelligently Controlled Cascade Injection Molding, *Kunststoffe international*, **1**, 2016, pp. 36-39.